Synthesis of Discrete Micrometer-Sized Spherical Particles of MCM-48

Carolina Petitto,[†] Anne Galarneau,*[,†] Marie-France Driole,[†] Bich Chiche,[†] Bruno Alonso,[‡] Francesco Di Renzo,[†] and François Fajula[†]

Laboratoire de Matériaux Catalytiques et Catalyse en Chimie Organique, UMR 5618 CNRS-ENSCM-UMI, Ecole Nationale Supérieure de Chimie de Montpellier, 8 rue de l'Ecole Normale, 34296 Montpellier Cedex 5, France, and CRMHT CNRS 1D, Avenue de la Recherche Scientifique, 45071 Orléans, France

Received January 12, 2005. Revised Manuscript Received February 9, 2005

The direct synthesis of a mesostructured silica with a tridimensional mesopore network with micrometer-sized and -shaped particles control is reported for the first time. Micrometer-sized beads of the cubic silica mesostructure MCM-48 have been obtained through a MCM-41 pseudomorphic synthesis procedure using preformed porous silica particles as silica source combined with a MCM-41/-48 phase transition. The low degree of polymerization of the MCM-41 formed in high alkaline conditions allows the further MCM-41/-48 phase transition. The kinetics of MCM-48 formation depends on the surface area of the parent silica, indicating that the dissolution of the silica in a confined environment is the rate-determining step of the process. The reaction time required to produce MCM-48 decreases from 7 to 2 h when the surface area of the parent silica increases from 160 to 740 m^2/g. The MCM-48 mesostructure is metastable toward a lamellar mesostructure at longer synthesis times (>20 h). The domain of existence of the different mesostructures as a function of synthesis time and surface area of the parent silica sources has been established. The aggregation state of the MCM-48 particles can be controlled by adjusting the dilution and the alkalinity of the synthesis medium.

Introduction

Due to their unique textural properties, micelle-templated silicas (MTS), such as MCM-41[1] disclosed in 1992, represent a class of promising supports for advanced separation processes. Their high surface area (ca. 900 m^2/g), high pore volume (ca. 0.7 mL/g), and adjustable pore size (between 2 and 15 nm) should improve, respectively, the retention capacity, the column permeability, and the molecular selectivity in a size-exclusion process. To test these hypotheses, great attention has to be paid to the control of the micrometric scale of MTS. Spherical particles with a narrow size distribution and without any aggregation are required for any significant chromatographic evaluation.[2] To reach the independent control of the nanometric and micrometric scales in MTS synthesis, we successfully developed a new strategy, named pseudomorphic synthesis,[3] that is based on the use of preformed porous silica spheres, commonly used as supports in chromatographic applications, as silica source in the synthesis of MCM-41. By using cetyltrimethylammonium bromide (CTAB) in alkaline media and optimized synthesis conditions, MCM-41 materials with pore diameters of 4 nm have been obtained as discrete and nonaggregated spheres of 5 or 10 μm. After surface modification by octylsilane chains, the grafted MCM-41 have been used as stationary phase in high performance reverse phase liquid chromatography (RP-HPLC) and led to great improvements in the separation process due to a lower resistance to mass transfer as compared to commercial silica gels.[4] The MCM-41 support allowed one to separate solutes faster than traditional commercial supports with higher column efficiency. In addition, their high surface area allows one to separate solutes that are not separated on classical column, by increasing their retention time, or to shorten the chromatographic column, for miniaturization purposes.

It is well known in the chromatographic community that the pore connectivity influences the column performance: a lower mass transfer resistance is expected for enhanced pore connectivity. To verify this assumption, micrometer-sized spherical particles of MCM-48, which has a higher pore connectivity as compared to MCM-41, represent the main objective of this work. MCM-48 features indeed a three-dimensional cubic structure, while MCM-41 is a two-dimensional hexagonal structure.[1] In addition, the control of the size, shape, and aggregation state of the MCM-48 particles is of prime importance for the development of these materials in chromatography.

MCM-48 mesoporous silicas remain largely undeveloped due to the difficulties encountered for their synthesis in terms

* To whom correspondence should be addressed. E-mail: galarne@cit.enscm.fr.
[†] Laboratoire de Matériaux Catalytiques et Catalyse en Chimie Organique.
[‡] CRMHT CNRS 1D.

(1) Beck, J. S.; Vartuli, J. C.; Roth, W. J.; Leonowicz, M. E.; Kresge, C. T.; Schmitt, K. D.; Chu, C. T.-W.; Olson, D. H.; Sheppard, E. W.; McCullen, S. B.; Higgins, J. B.; Schlenker, J. L. *J. Am. Chem. Soc.* **1992**, *114*, 10834.
(2) Coulson, J. M. *Trans. 1nst. Chem. Eng.* **1949**, *27*, 237.
(3) Martin, T.; Galarneau, A.; Di Renzo, F.; Fajula, F.; Plee, D. *Angew. Chem., Int. Ed.* **2002**, *41*, 2590.
(4) Martin, T.; Galarneau, A.; Di Renzo, F.; Brunel, D.; Fajula, F.; Heinisch, S.; Cretier, G.; Rocca, J.−L. *Chem. Mater.* **2004**, *16*, 1725.

10.1021/cm050068j CCC: $30.25
Published on Web 03/23/2005

of reproducibility and synthesis yield. The first synthesis of MCM-48 has been performed in the presence of cetyltrimethylammonium as surfactant (CTMA)[1,5] and tetraethoxysilane (TEOS) as silica source. Yet it was shown that CTMA was more favorable for the synthesis of the hexagonal phase (MCM-41) by forming cylindrical micelles.[6,7] To synthesize MCM-48, it has been shown that ethanol (added in the synthesis or formed during TEOS hydrolysis)[8−10] was useful to avoid the growth of cylindrical micelles by increasing the surfactant packing parameter.[6,11] The reproducibility of MCM-48 synthesis was improved some years later by using gemini dicationic surfactants without organic cosurfactant.[12,13] Gemini surfactants were found to favor the formation of MCM-48 even without organic additives and using fumed silica as silica source.[14] New strategies of MCM-48 synthesis were also introduced, based on the use of mixtures of cationic and nonionic surfactants.[15,16] MCM-48 materials were synthesized by using mixtures of alkyltrimethylammonium bromides and polyoxyethylene alkyl ethers, with sodium silicate as the silica source.[16] Very few syntheses have used solid silica as silica source. Fumed silica and CTAB as surfactant without any addition of alcohol as cosurfactant have been used in only two previous studies.[17,18]

The preparation of nonaggregated spherical particles with controlled sizes in the micrometer range (5, 10 μm or larger) adds a further challenge to the synthesis of MCM-48. Spherical particles of MCM-48 in the nanometer range (200−700 nm) have been synthesized from water−alcohol systems by using ethanol as cosolvent and ammonia as catalyst in modified Stöber conditions in diluted media.[19,20] To use these nanoparticles in chromatography, further agglomeration has been performed using a spray drying technique to obtain micrometric spherical particles.[21] The particle size distribution of the resulting materials is quite broad between 10 and 20 μm, which required further sizing. One main limitation of this multistep procedure is the high dilution of the nanoparticles synthesis media, which results in very poor yields.

Recently, Xia et al.[22] have shown that MCM-48 mesoporous silica may be obtained using fumed silica and CTMAOH through phase transition from the hexagonal MCM-41 mesostructure in 24 h at 135 °C. Several authors have observed the phase transition of the hexagonal phase MCM-41 into the cubic phase MCM-48 in syntheses made by using TEOS as silica source.[8,23,24] Gallis and Landry[8] synthesized MCM-48 from MCM-41 by a phase transition obtained by heating an incompletely polymerized mesostructure to 150 °C. The authors claimed that ethanol, produced during TEOS (silica source) hydrolysis, was responsible for the phase transition process by increasing the surfactant packing parameter. However, the synthesis of MCM-48 by a phase transition has also been observed under different synthesis conditions and by using different silica sources: fumed silica[18,22] and sodium silicate[25,26] without adding ethanol. The MCM-41/-48 phase transition has similarities to the transition of the analogous liquid-crystal systems (surfactant/water) of the hexagonal H_α phase and the cubic Q_α phase. XRD and neutron scattering experiments have shown a geometric correlation between the [10] plane of the H_α phase and the [211] planes of the Q_α phase. In the mesostructure system (surfactant/water/silica), the MCM-41/-48 phase transition will take place, if a low degree of silica polymerization is observed.[8,27] This condition implies a high alkaline medium, a high surfactant concentration, or the presence of ethanol to slow silicate polymerization. A high-temperature synthesis between 130 and 170 °C, which usually increases the condensation state of silica, acts as a booster of phase transition kinetic. In general, longer stirring times and shorter heating times are essential for the successful synthesis of MCM-48 at the highest temperature; otherwise the more favorable lamellar phase or a mixture of lamellar and cubic phases is obtained.

In this work, we present how micrometer-sized spherical particles of MCM-48 can be synthesized from CTAB surfactants in alkaline conditions by the control of different kinetic parameters governing the MCM-41/-48 phase transition through a pseudomorphic synthesis using different amorphous silica beads as silica source.

Experimental Section

Materials. MCM-48 mesostructures were synthesized by using cetyltrimethylammonium bromide (CTAB) from Aldrich as surfactant and from different sources of silica, a nonporous fumed silica (Aerosil 200 from Degussa), and spherical beads of porous silicas traditionally used as chromatography supports, LiChrospher 60 (Merck), Nucleosil 100-5 (Macherey-Nagel), Hypersil (Thermoquest Inc.), and SiMatrex 60 (Amicon). The textural features of the silica precursors were reported in Table 1. To synthesize MCM-48 mesostructures, a first solution of CTAB in alkaline solution was

(5) Kresge, C. T.; Leonowicz, M. E.; Roth, W. J.; Vartuli, J. C.; Beck, J. S. *Nature* **1992**, *359*, 710.
(6) Huo, Q.; Margolese, D. I.; Stucky, G. D. *Chem. Mater*. **1996**, *8*, 1147.
(7) Morey, M. S.; Davidson, A.; Stucky, G. D. *J. Porous Mater*. **1998**, *5*, 195.
(8) Gallis, K. W.; Landry, C. C. *Chem. Mater*. **1997**, *9*, 2035.
(9) Lebedev, O.; Van, T.; Collart, O.; Cool, P.; Vansant, E. F. *Solid State Sci.* **2004**, *6*, 489.
(10) Kim, J. M.; Kim, S. K.; Ryoo, R. *Chem. Commun*. **1998**, 259.
(11) Monnier, A.; Schüth, F.; Huo, Q.; Kumar, D.; Margolese, D. I.; Maxwell, R. S.; Stucky, G. D.; Krishnamurty, M.; Pertroff, P.; Firouzi, A.; Janicke, M.; Chmelka, B. F. *Science* **1993**, *261*, 1299.
(12) Huo, Q.; Leon, R.; Petroff, P. M.; Stucky, G. *Science* **1995**, *268*, 1324.
(13) Van Der Voort, P.; Mathieu, M.; Mees, F.; Vansant, E. F. *J. Phys. Chem. B* **1998**, *102*, 8847.
(14) Collart, O.; Van der Vort, P.; Vansant, E. F.; Desplantier, D.; Galarneau, A.; Di Renzo, F.; Fajula, F. *J. Phys. Chem. B* **2001**, *105*, 12771.
(15) Chen, F.; Huang, L.; Li, Q. *Chem. Mater*. **1997**, *9*, 2685.
(16) Ryoo, R.; Joo, S. H.; Kim, J. M. *J. Phys. Chem. B* **1999**, *103*, 7435.
(17) Corma, A.; Kan, Q.; Rey, F. *Chem. Commun.* **1998**, 579.
(18) Sayari, A. *J. Am. Chem. Soc*. **2000**, *122*, 6504.
(19) Schumacher, K.; Grun, M.; Unger, K. K. *Microporous Mesoporous Mater*. **1999**, *27*, 201.
(20) Lebedev, O. I.; Van Tendeloo, G.; Collart, O.; Cool, P.; Vansant, E. F. *Solid State Sci.* **2004**, *6*, 489.
(21) Lind, A.; du Fresne von Hohenesche, C.; Smatt, J. H.; Lindén, M.; Unger, K. K. *Microporous Mesoporous Mater*. **2003**, *66*, 219.
(22) Xia, Y.; Mokaya, R.; Titman, J. J. *J. Phys. Chem. B* **2004**, *108*, 11361.
(23) Romero, A. A.; Alba, M. D.; Zhou, W.; Klinowski, J. *J. Phys. Chem. B* **1997**, *101*, 5294.
(24) Xu, J.; Luan, Z.; He, H.; Zhou, W.; Kevan, L. *Chem. Mater*. **1998**, *10*, 3690.
(25) Liu, Y.; Karkamkar, A.; Pinnavaia, T. J. *Chem. Commun.* **2001**, 1822.
(26) Diaz, I.; Perez-Pariente, J.; Terasaki, O. *J. Mater. Chem.* **2004**, *14*, 48.
(27) Landry, C. C.; Tolbert, S. H.; Gallis, K. W.; Monnier, A.; Stucky, G. D.; Norby, P.; Hanson, J. C. *Chem. Mater.* **2001**, *13*, 1600.

Table 1. Morphology and Textural Features (Particle Size, Surface Area (S_{BET}), Primary Nanoparticles Size (d_{np}), Pore Volume (V), Pore Diameter (D)) of the Chromatographic Parent Silicas Used as Silica Sources in the MCM-48 Synthesis with Morphology Control

silicas	particle shape	particle size (μm)	S_{BET} (m^2/g)	d_{np} (nm)	V (mL/g)	D (Å)
LiChrospher 60	sphere	12	743	4	0.77	60
Nucleosil 100-5	sphere	5	372	7	1.17	150
Hypersil	sphere	5	160	17	0.61	165
SiMatrex 60	shards	5	600	5	1.07	85

prepared and stirred at 50 °C in a stainless steel autoclave. The silica source was then added to this solution under stirring to give gel mixtures with the molar compositions $1SiO_2/0.30-0.38NaOH/0.175CTAB/120-160H_2O$. After 2 h of stirring at 50 °C, the autoclave was sealed and heated at 150 °C for different periods of time under static conditions. The solid precipitate was then recovered by filtration, washed with deionized water, and dried at 80 °C overnight.

Characterization. Powder X-ray diffraction (XRD) data were obtained on a Bruker AXS D8 diffractometer by using Cu Kα radiation and a Ni filter. The adsorption/desorption isotherms of nitrogen at 77 K were measured using a Micromeritics ASAP 2010 instrument. The as-synthesized mesostructures were calcined in flowing air at 550 °C for 8 h and stored under ambient conditions prior to analysis. Each calcined sample was outgassed at 250 °C until a stable static vacuum of 3×10^{-3} Torr was reached. The mesopore diameter was calculated from the desorption branch of nitrogen isotherms by the Broekhoff and de Boer (BdB) method,[28] which has been shown to provide reliable results for MCM-41 materials.[29] Special care was taken in the determination of the BET specific surface area, that is, to calculate the linearization of the BET equation by avoiding points at low pressure affected by heterogeneity of surface and points at high pressure corresponding to the start of pore filling. Pore volumes were calculated at the end of the step corresponding to the filling of the pores. Thermogravimetric analyses (TGA) were performed using a Netzsch TG209C balance. The heat rate was maintained at 5 °C/min in air flow up to 850 °C. Yields (in mol %) of the syntheses were expressed as (amount of element in the as-synthesized dried solid/total amount of element in the gel) × 100. Scanning electron microscopy (SEM) images were obtained using a Hitachi apparatus after platinum metalation of the samples. ^{29}Si MAS NMR was performed on an ASX Bruker NMR spectroscope with 9.4 T field and 6 kHz MAS. ^{13}C MAS NMR spectra were recorded on a Bruker DSX 400 spectrometer by means of 2.5 mm MAS rotors spun at 30 kHz. Radio frequency fields of 50 kHz were employed. Spectra were referenced to TMS. Particle size distributions were recorded on a Malvern MASTER SIZER 2000: 200 mg of sample was added to 50 mL of water and ultrasons were used for 2 min, before diluting the suspension into 700 mL of water for analysis.

Results and Discussion

MCM-48 Synthesis from Nonporous Silica. Before using preformed porous silica spheres as silica source for the synthesis of MCM-48, the experimental conditions leading to the cubic mesostructure were established by using the nonporous powder silica, fumed silica (Aerosil 200). At 150 °C, pure MCM-48 was obtained after 4 h of reaction, starting from gels with the following molar composition: $1SiO_2/0.38NaOH/0.175CTAB/120H_2O$. The XRD pattern for the as-synthesized MCM-48 is shown in Figure 1a (middle) and showed the (211) and (220) diffraction peaks at low 2θ angles characteristic of the *Ia*3*d* space group. Under the very same experimental conditions, 2.5 h of reaction produced the MCM-41 mesostructure, identified by the characteristic (100), (110), and (200) XRD peaks of the hexagonal symmetry (space group *p*6*mm*, Figure 1a, top). Finally, the same gel composition heated for 20 h led to the lamellar mesostructure featuring two XRD peaks corresponding to planes (100), at 33 Å, and (200), at 15.5 Å. Thermogravimetric analysis reveals that ca. 90% of surfactant and ca. 80% of silica are incorporated in all mesostructures. This indicates that the samples are formed by mesostructures.

The three different mesostructures are clearly identified in the SEM pictures shown in Figure 1b. Actually, MCM-41, MCM-48, and the lamellar mesostructures exhibit rather different morphologies. The parent nonporous silica is formed of 15 nm primary particles in very loose aggregates. The nucleation and growth of MCM-41 give rise to aggregates (7−14 μm) of distorted elongated crystals 1−3 μm in size, with dispersed smaller particles probably formed by secondary nucleation. The subsequently formed MCM-48 presents the morphology of icosahedral crystals up to 1 μm in size. The crystals form raspberry-like hollow aggregates, 3−4 μm large. The lamellar mesostructure is built by the loose association of thin platelets of 100 nm thickness and 3−4 μm width.

The MCM-41/-48 phase transition has been already reported by several groups, but for different synthesis times. For instance, using fumed silica as silica source, Xia et al.[22] observed full transformation of MCM-41 into MCM-48 after 24 h of reaction at a synthesis temperature of 135 °C, instead of 4 h in our synthesis conditions performed at 150 °C. Extensive hydrothermal treatment, 36 h at 150 °C, has been also required by Liu et al.[25] to achieve the transformation in the presence of sodium silicate as the silica source. By contrast, starting from mixtures prepared from silicon alkoxides and under experimental conditions and gel compositions very similar to those reported here, Landry et al.[27] and Tolbert et al.[30] observed a faster MCM-41/-48 phase transformation (ca. 2 h). In both studies, in-situ XRD experiments revealed a transient formation of the lamellar phase at the beginning of the transformation, that, depending on the conditions of preparation of the gel at room temperature, either vanished[27] or developed[30] upon heating. The diversity of the situations encountered clearly indicates very complex phase behaviors where the very same mesostructure may be formed under either kinetic or thermodynamic control. In our case, no lamellar mesostructure could be identified at short synthesis times. Under our conditions, therefore, MCM-48 forms as a metastable product between the kinetically favored MCM-41 mesostructure and the more thermodynamically stable lamellar phase. Such a sequence has also been reported by Xia et al.[22] Several comprehensive explanations have been proposed to describe the mechanism of the phase transformation of mesostructured silicas. Although the exact nature of the driving force of the process is still a matter of debate, it

(28) Broekhoff, J. C. P.; De Boer, J. H. *J. Catal.* **1968**, *10*, 377.
(29) Galarneau, A.; Desplantier, D.; Dutartre, R.; Di Renzo, F. *Microporous Mesoporous Mater.* **1999**, *27*, 297.
(30) Tolbert, S. H.; Landry, C. C.; Stucky, G. D.; Chmelka, B. F.; Norby, P.; Hanson, G. C.; Monnier, A. *Chem. Mater.* **2001**, *13*, 2247.

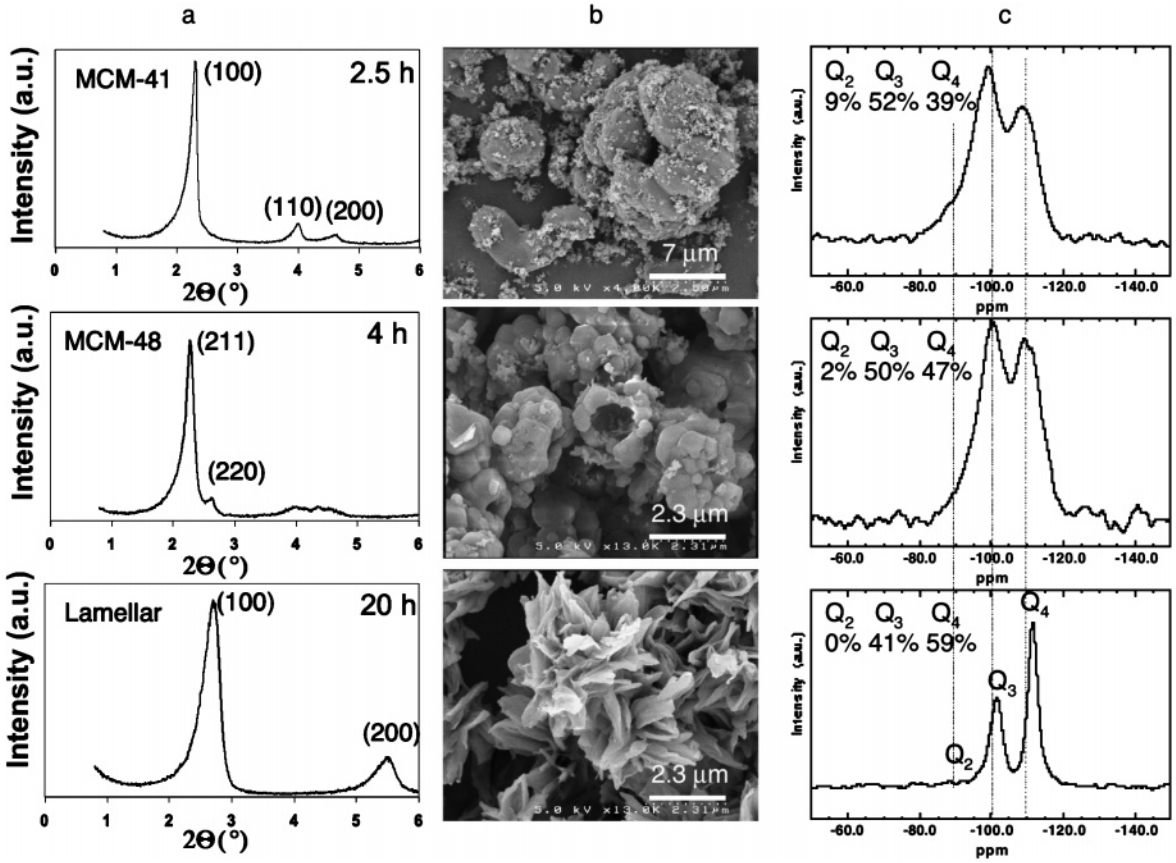

Figure 1. (a) XRD pattern, (b) SEM pictures, and (c) ^{29}Si MAS NMR of as-synthesized MCM-41, MCM-48, and lamellar mesostructures obtained from fumed silica as silica source and at different synthesis times at 150 °C of 2.5, 4, and 20 h, respectively.

seems agreed that the transformation is governed by the rearrangement of the organic fraction of a hybrid mesostructure where the inorganic region is scantly polymerized.

The ^{29}Si MAS NMR spectra (Figure 1c) confirmed the low degree of polymerization silica for MCM-41 and MCM-48 in our synthetic conditions. Deconvolution of the NMR signals led to 9% of Q_2 ($(SiO)_2Si(OH)_2$ at −88.5 ppm), 52% of Q_3 ($(SiO)_3Si(OH)$ at −98.5 ppm), and 39% of Q_4 ($(SiO)_4Si$ at −109.1 ppm). In MCM-41 mesostructures synthesized in lower alkaline media ($OH^-/SiO_2 = 0.25$), like in our previous pseudomorphic synthesis of MCM-41,[3] no MCM-41/-48 phase transition was observed and the percentage of fully condensed tetrahedra (siloxane (Q_4)) was classically 60−70% instead of less than 40% like in the present syntheses performed at higher alkalinity ($OH^-/SiO_2 = 0.38$). The ^{29}Si MAS NMR spectrum of MCM-48 is very similar to that of MCM-41, with a slightly higher condensation degree of the silicate species with 2% of Q_2 at −90.7 ppm, 50% of Q_3 at −99.8 ppm, and 47% of Q_4 at −110.0 ppm. The resulting as-synthesized MCM-48 mesostructures present nevertheless a poorly condensed network and lead to strong restructurization during calcination. One possibility to limit this restructurization consists of enhancing the degree of silica condensation before calcination by applying a subsequent hydrothermal posttreatment.[14,31] The ^{29}Si MAS NMR spectrum of the lamellar mesostructure (Figure 1c, bottom) presents somewhat different features as compared to the MCM-41 and MCM-48 spectra. The ^{29}Si MAS NMR spectrum of the lamellar mesostructure is composed of two peaks corresponding to 41% of Q_3 at −101.3 ppm and 59% of Q_4 at −111.5 ppm. These figures show that the inorganic fraction in the lamellar phase is more polymerized and/or reticulated than in the hexagonal and cubic phases. Moreover, the width of the NMR signals equals 4 ppm, while 9 ppm wide peaks were measured for MCM-41 and MCM-48. The local structure of the silicate fraction in MCM-41 and MCM-48 appears therefore as very close in terms of hydroxylation state and bonding, whereas a more condensed system prevails in the lamellar mesostructure.

A similar discrimination between the various phases was revealed for the organic fraction from ^{13}C MAS NMR measurements of the occluded surfactant (Figure 2). The ^{13}C NMR resonance lines of alkylammonium moieties entrapped in porous silicas can be divided into two families: (i) a group of narrow lines due to carbon groups along the chain (from C4 to C16) and the methyl C1 and C17; and (ii) a family of broad peaks due to the polar group for C2 and C3. The methylene carbon directly bonded to nitrogen C2 expected at 68 ppm is not visible in the three mesostructures, which is characteristic of a restricted mobility of the surfactant head anchored onto the silicate surface.[32] Also, the methylene C3 suffers from this limited mobility and is not visible for the MCM-41 and MCM-48 mesostructures. By contrast, the

(31) Galarneau, A.; Driole, M. F.; Petitto, C.; Chiche, B.; Bonelli, B.; Armandi, M.; Onida, B.; Garrone, E.; di Renzo, F.; Fajula, F. *Microporous Mesoporous Mater*. **2005**, in press.

(32) Simonutti, R.; Comotti, A.; Bracco, S.; Sozzani, P. *Chem. Mater*. **2001**, *13*, 771.

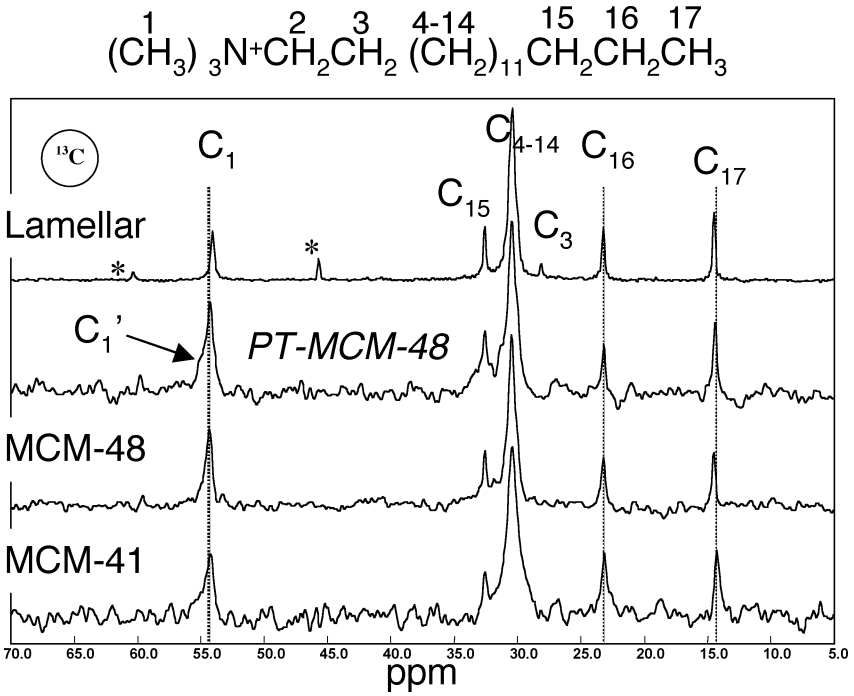

Figure 2. ^{13}C MAS NMR of as-synthesized MCM-41, MCM-48, and lamellar mesostructures obtained from nonporous silica (Aerosil 200) as silica source and at different synthesis times at 150 °C of 2.5, 4, and 20 h, respectively.

other carbon atoms of the surfactant exhibit intense and narrow signals. The alkyl chains of CTMA surfactants in MCM-41 and MCM-48 hardly interact therefore with the silica network; they are less mobile than in solution, but they are more mobile than in an ordered well-condensed MCM-48 produced by hydrothermal posttreatment (PT-MCM-48 in Figure 2),[14,31] which features an additional C1′ resonance at 57.4 ppm characteristic of a lower mobility surfactant in an ordered mesostructure.[33] This fact confirms the mobility of the surfactants, which allows the inner organic matter to drive the MCM-41/-48 phase transition. The appearance of the methylene C3, the increase of the signal-to-noise ratio, as well as the slight high-field shift for the methyl groups next to the headgroup (C1)[33] for the lamellar mesostructure are all characteristic of a slight increase of surfactant mobility, due to a less confined space.

Our results, as well as literature reports, conclusively show that the observed phase transitions arise from a cooperative rearrangement of the surfactant micelles and a poorly condensed silicate gel following mechanisms that may not be unique. Time-resolved variable-temperature in-situ XRD experiments show, for instance, that, depending on the heating profile, mesostructure transformations may proceed according to discontinuous or to continuous or epitaxial transitions.[27,30] In addition, the nature of the parent silicate source appears as a critical parameter in determining the kinetics of the process. It can be anticipated that this situation finds its origin in the reactivity of the silicate source. Such a parameter is hardly considered in the literature for MCM-48, as only three sources of silica (TEOS, sodium silicates, and fumed silica) have been used for its synthesis. It should prove of prime relevance with regards to our objective to produce MCM-48 beads from several preformed silicas, as will be discussed below.

MCM-48 Synthesis from Porous Preformed Silicas. *Pseudomorphic Synthesis Combined with MCM-41/-48 Phase Transition.* Pseudomorphism is the accepted mineralogical term for a phase transformation in which the macroscopical shape of the material is retained. In the field of mesostructured materials, the pseudomorphic synthesis has been defined as the transformation of amorphous silica bead in a silica-surfactant mesostructure without any modification of the shape and size of the bead.[3] The process is controlled by the dissolution of the amorphous silica to provide the inorganic component of the silica-surfactant mesostructure and requires that the pore volume of the parent silica can accommodate the volume expansion resulting from the phase transformation. The pseudomorphic synthesis has been successfully applied to the production of well-ordered spherical particles of MCM-41 (40 Å mesopore size)[3] of 5, 10, and 50 μm diameter and to the synthesis of spherical particles (10 μm diameter) of micelle-templated silicas with larger pores (in the range 60−90 Å).[34] In these previous works, the initial silica particles played the role of discrete nanoreactors inside which all of the reaction occurred. No formation of mesostructure in the solution phase nor aggregation between the particles was observed. In the present work, the pseudomorphic synthesis was used to obtain MCM-41 with low degree of silica polymerization as in the procedure developed above from gels prepared from nonporous silica, to expect a MCM-41/-48 phase transition without particle morphology changes. The synthesis of spherical particles of MCM-48 by this procedure has been applied to various preformed silica particles starting from a

(33) Wang, L. Q.; Liu, J.; Exarhos, G. J.; Bunker, B. C. *Langmuir* **1996**, *12*, 2663.

(34) Lefèvre, B.; Galarneau, A.; Iapichella, J.; Petitto, C.; Di Renzo, F.; Fajula, F.; Bayram-Halm, Z.; Skudas, R.; Unger, K. *Chem. Mater.* **2005**, *17*, 601.

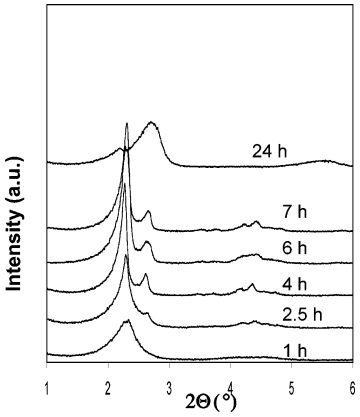

Figure 3. XRD pattern within time of the synthesis using LiChrospher 60 as parent silica. In 1 h of synthesis, MCM-41 is formed. From 2 to 7 h, MCM-48 is obtained. In 24 h of synthesis, lamellar mesostructure is obtained alongside some traces of MCM-48.

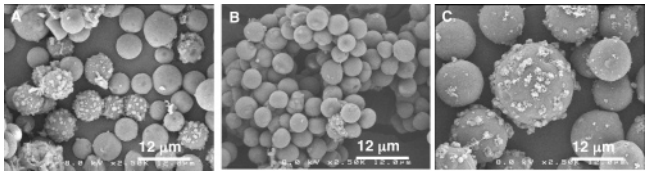

Figure 4. SEM pictures of spherical particles of MCM-48 obtained from different silica sources: (A) from Hypersil, 15 h synthesis (120 H_2O/Si), (B) from Nucleosil, 6 h synthesis (120 H_2O/Si), and (C) from LiChrospher 60, 15 h synthesis time (160 H_2O/Si).

gel with the overall molar ratio composition $1SiO_2$/0.38NaOH/0.175CTAB/120H_2O and a temperature of synthesis of 150 °C. Relevant characteristics of the different silica sources, LiChrospher 60, Nucleosil 100-5, Hypersil, and SiMatrex 60, are reported in Table 1. All preformed silicas are stationary phases used for chromatography applications. Their pore size varies between 60 and 170 Å, their surface areas vary from 160 to 740 m^2/g, and their pore volume varies from 0.6 to 1.2 mL/g. The difference in the textural properties of the preformed silicas originates from the different size and packing of the primary nanoparticles constituting the silica particles.[35] The silica samples have been chosen on the basis of their pore volume, required to be large enough to accommodate the increase of pore volume developed during the transformation from amorphous silica to silica-surfactant mesostructure.

The kinetics of phase transformation have been followed by XRD and SEM. Basically the same sequence of mesostructure formation, hexagonal/cubic/lamellar, and the trends discussed above in the experiments performed with nonporous silica were observed with all preformed porous silica sources. For instance, in Figure 3 are reported the XRD patterns as a function of reaction time for the synthesis performed using LiChrospher 60. The *d*-spacings and unit cell parameters are reported in Table 2. At short synthesis time (1 h), a MCM-41 mesostructure is formed with a *d*-spacing of $d_{100} = 39$ Å. From 2 to 7 h of reaction, well-defined MCM-48 mesostructures are obtained with a *d*-spacing of $d_{211} = 39$ Å corresponding to a cell parameter of 95 Å. At a longer synthesis time (24 h), the lamellar phase

(35) Ramsay, J. D. F.; Russell, P. J.; Swanson, S. W. *Stud. Surf. Sci. Catal.* **1991**, *62*, 257.

Table 2. XRD Features and Synthesis Molar Yields of As-Synthesized Mesostructures Obtained by Pseudomorphic Synthesis during Different Synthesis Times at 150 °C Using LiChrospher 60 as Parent Silica and a Gel Molar Composition of $1SiO_2$/0.38NaOH/0.175CTAB/120H_2O

time (h)	meso-structure	*d*-spacing first peak (Å)	unit cell (Å)	$yield_{CTMA}$[a] (%)	$yield_{Si}$[b] (%)	CTMA/Si
1	hexagonal	38.6	44.6	72	62	0.237
1.5	hexagonal	37.0	42.7	81	67	0.240
2	cubic	37.9	92.8	85	70	0.245
2.5	cubic	38.6	94.5	83	71	0.240
3	cubic	38.8	94.9	90	71	0.260
4	cubic	39.1	95.8	87	66	0.267
5	cubic	38.8	95.0	88	68	0.264
6	cubic	38.5	94.4	82	62	0.270
7	cubic	38.5	94.4	82	70	0.240
24	lamellar	32.9		81	77	0.210
	(+cubic traces)	40.1				

[a] Yield of CTMA. [b] Yield of silica.

Table 3. ^{29}Si MAS NMR Data of As-Synthesized Mesostructures Obtained through Pseudomorphic Synthesis during Different Synthesis Times at 150 °C Using LiChrospher 60 as Parent Silica and a Gel Molar Composition of $1SiO_2$/0.38NaOH/0.175CTAB/120H_2O

		Q_2		Q_3		Q_4	
time (h)	mesostructure	ppm	%	ppm	%	ppm	%
1	hexagonal	−89.4	7	−99.1	49	−109.2	44
2.5	cubic	−90.0	8	−99.2	48	−109.2	44
4	cubic	−88.4	9	−99.5	44	−109.3	47
6	cubic	−89.8	6	−98.9	48	−108.9	46
7	cubic	−89.5	7	−99.0	49	−109.0	46
24	lamellar		0	−101.2	47	−111.7	53

appears with the characteristic peaks at $d_{100} = 33$ Å and $d_{200} = 15.5$ Å. Traces of the MCM-48 mesostructure are still present along with the lamellar phase, as evidenced by a small peak at a *d*-spacing of 40 Å. ^{29}Si MAS NMR measurements confirmed a low degree of condensation of the silicates (in the range of 45% Q_4) for the hexagonal and cubic phases (Table 3) and a higher level of reticulation (around 55% Q_4) for the lamellar phase. As regards the shape of the mesostructures obtained through pseudomorphic synthesis procedure combined with MCM-41/-48 phase transition, SEM pictures (Figure 4) show the preservation of spherical shape and particle size of the parent silica particles.

The retention of the overall morphology for MCM-41 and MCM-48 (Figure 5) indicates that MCM-41 is formed by pseudomorphic transformation and MCM-48 by phase transition inside the MCM-41 beads and that their nucleation and growth occur inside the particles through short-range transport mechanism. MCM-41 spheres formed after 1 h of synthesis are composed of MCM-41 nanocrystals or nanodomains and have the same appearance as the particles of the parent silica.[3] Some elongated MCM-41 crystals can be observed at the surface of the particles (Figure 5). The growth of elongated crystals situated at the outer surface of the spheres has already been observed in the pseudomorphic synthesis of MCM-41 at lower temperature (115 °C) for a longer synthesis time (1 month) or for very alkaline media in poor-surfactant systems (CTMA/Si = 0.10).[3] The MCM-48 spheres formed at 2.5 and 4 h of synthesis time can be surrounded by a shell formed by 1 μm of smooth icosahedra (Figure 5) coming from the MCM-41/-48 phase transition of the previous elongated MCM-41 crystals found at the outer

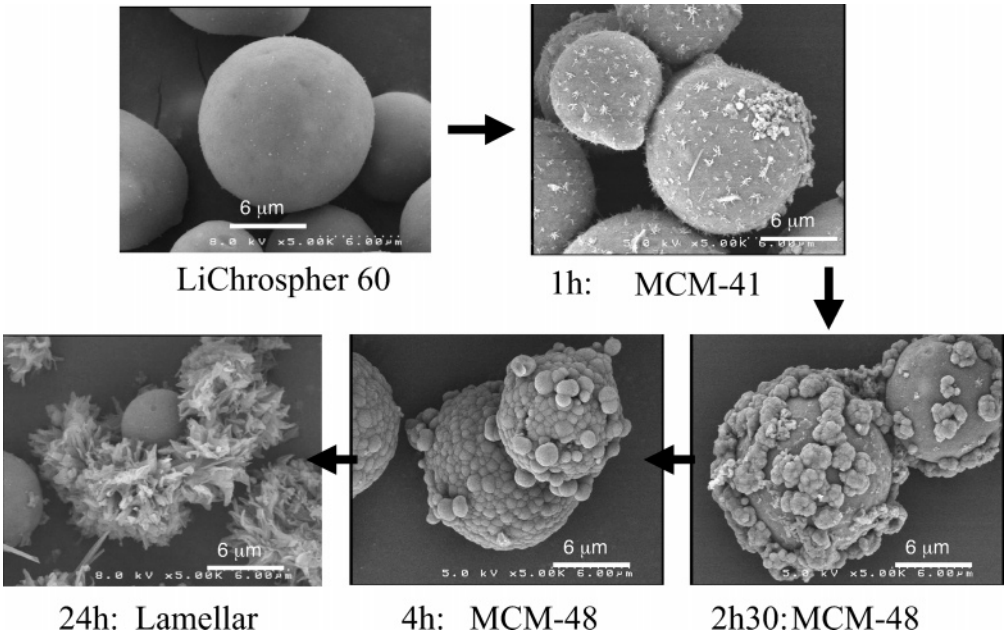

Figure 5. SEM pictures of LiChrospher 60 and its following pseudomorphic transformation going through MCM-41 mesostructure in 1 h of synthesis, MCM-48 mesostructure in 2.5 and 4 h of synthesis, and lamellar mesostructure in 24 h of synthesis. The particle morphology and size of the initial parent silica is preserved for MCM-41 and MCM-48. In some MCM-48 particles, an additional shell around the particle is formed.

surface of MCM-41 particles. X-ray diffraction (Figure 3) indicates that the transformation MCM-41/-48 has been completed; hence the core of the spheres is also formed by MCM-48 particles of smaller crystals or domains size. The location of the largest crystals or domains of MCM-48 at the outer surface of the spheres suggests that the nucleation of MCM-48 has occurred first at the rim of the MCM-41 spheres. It is likely that the outer crystals are the largest ones because they had a longer growth time. The presence of crystals or domains with different size in the particle is the driving force for an Ostwald ripening mechanism: the largest crystals or domains of MCM-48 grow at the expense of the smallest ones, which have a higher solubility,[36] increasing the difference in size. This mechanism leads progressively to the partial dissolution of the core of the MCM-48 spheres, with the separation of the outer shell from the core of the particles (Figure 6).

At difference with the pseudomorphic formation of MCM-41 and the following phase transition into MCM-48, the formation of the lamellar phase does not imply any short-range transport mechanism or solid-state phase transition. Indeed, the morphology of the lamellar structure obtained after 24 h of synthesis is similar to that found with nonporous silica as parent silica: disordered aggregates of thin plates throughout the whole material with no trace of the initial parent spherical morphology. It seems clear that the lamellar phase nucleation is not epitaxial, but that nucleation takes place in solution from the excess of silicates present in solution. The lamellar phase forms a more stable phase due to its higher condensation state of silicates featured by 53% of Q_4 (Table 3), and its growth induces the dissolution of the less stable (less condensed) MCM-48 mesostructure.

Changes in Textural Characteristics and Composition during MCM-41 Pseudomorphic Synthesis Followed by MCM-41/-48 Phase Transition. The evolution of the textural properties of the mesostructures as a function of the synthesis time at 150 °C has been followed by nitrogen sorption at 77 K on the calcined materials (Figure 7). The nitrogen adsorption−desorption of the parent silica, LiChrospher 60, has been given as reference. After 1 h of synthesis, the parent silica is completely transformed into MCM-41. All of the broadly distributed mesoporosity of the starting silica is lost and transformed into the ordered porosity of MCM-41. The MCM-41 formed presents a poorly condensed silica framework (Table 3) and underwent a strong restructurization during calcination with a unit cell contraction of 10 Å (20%) from 45 to 35 Å (Tables 2 and 4), which gives rise to a calcined MCM-41 material with a low pore volume and small pore size (25 Å).

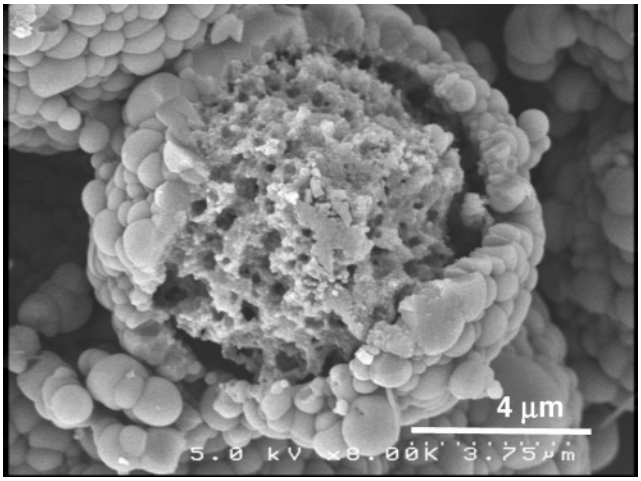

Figure 6. SEM pictures of MCM-48 particle obtained from LiChrospher 60 as parent silica in 7 h of synthesis revealing some holes in the core of the particle and the separation of the shell.

In the case of the MCM-48 phase formed at a later stage, the unit cell shrinking upon calcination is about 16 Å (15%) from 95 to 79 Å. MCM-48 presents a remarkable constancy

(36) Finsy, R. *Langmuir* **2004**, *20*, 2975.

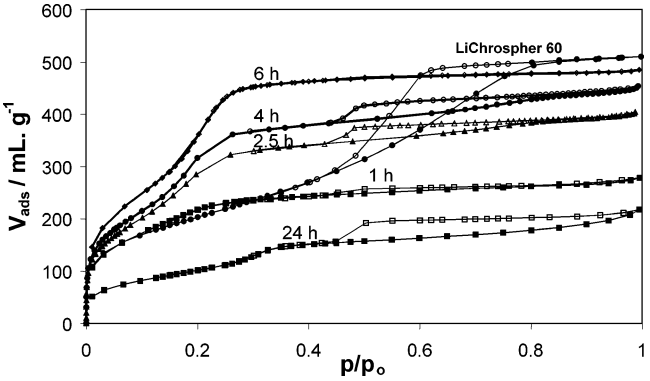

Figure 7. Nitrogen adsorption−desorption isotherms at 77 K of calcined at 550 °C mesostructures obtained within time through the pseudomorphic transformation of LiChrospher 60 into MCM-41 in 1 h of synthesis, MCM-48 from 2.5 to 6 h, and into lamellar phase with some traces of MCM-48 in 24 h of synthesis. The LiChrospher 60 nitrogen isotherm is given as reference.

Table 4. XRD and Textural Features (Pore Volume (V_p), BET Surface Area (S_{BET}), Pore Diameter (D), Wall Thickness (t)) of Calcined Mesostructures Obtained by Morphology Control Synthesis during Different Synthesis Times at 150 °C Using LiChrospher 60 as Parent Silica and Calcined at 550 °C for 8 h

time (h)	meso-structure	*d*-spacing first peak (Å)	unit cell (Å)	V_p (mL/g)	S_{BET} (m^2/g)	D (Å)	t (Å)
1	hexagonal	30.0	34.7	0.36	843	25	11
1.5	hexagonal	30.2	34.9	0.76	1542	26	10
2	cubic	32.2	78.8	0.59	1534	26	12
2.5	cubic	31.3	76.7	0.51	1099	26	12
3	cubic	32.3	78.9	0.62	1326	28	12
4	cubic	31.7	77.6	0.56	1199	27	12
5	cubic	32.2	78.9	0.58	1176	28	12
6	cubic	32.0	78.4	0.71	1478	28	11
7	cubic	32.0	78.4	0.71	1365	28	11
24	lamellar			0.23	377	34	
	(+cubic traces)	36.8					

of diffraction parameters throughout the synthesis, both in the as-synthesized and in the calcined form. However, some textural evolution takes place during the synthesis. The pore volume of the calcined MCM-48 increases when the synthesis time increases (6−7 h). The apparent contradiction between the constancy of the diffraction parameters and the evolution of the textural characteristics as a function of synthesis time is more likely due to a lack of stability during calcinations, which could be due either to the core/shell nature of the MCM-48 mesostructure or to the growth of MCM-48 domains inside the particle. At longer synthesis times, a larger portion of the MCM-48 mesostructure is constituted of large well-ordered smooth icosahedral crystals and/or larger domains inside the particle with improved resistance upon calcination. This will affect little the XRD patterns, which are dominated by the contribution of the largest crystals and/or domains since the very beginning of their formation, but will significantly impact pore volumes. After 6 h of synthesis, MCM-48 materials have a pore volume of 0.70 mL/g, pore diameter of 28 Å, and a surface area of 1400 m^2/g. A limited volume of secondary porosity (hysteresis loop closed near p/p_0 0.45 in Figure 7) is observed in some MCM-48 materials, possibly due to cracks developed in the material during the calcination process. The decrease of the pore volume from 0.70 to 0.23 mL/g for 24 h of synthesis time is correlated with the formation of the lamellar

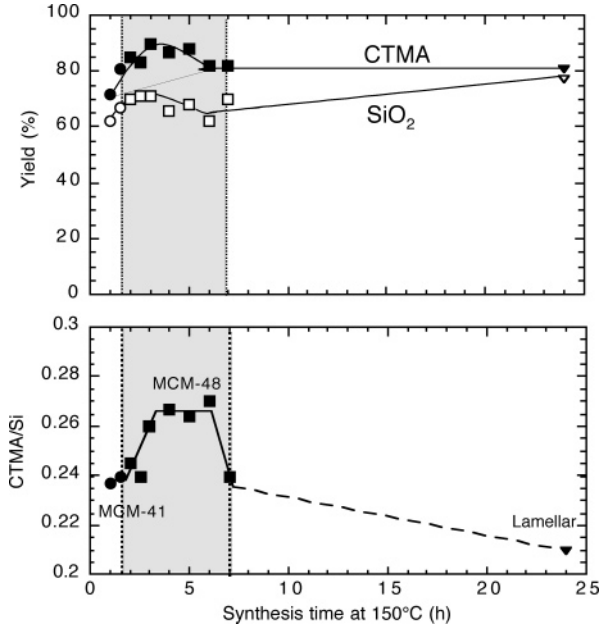

Figure 8. Molar percentage of silica and surfactant yields as well as CTMA/silica molar ratio as a function of the synthesis time. Each mesostructure is represented by circles for MCM-41, squares for MCM-48, and triangles for lamellar phase. The gray zone represents the MCM-48 domain.

phase, which collapses upon calcination. Nevertheless, the observed porosity is due to some remaining cubic phase as identified by XRD (Figure 3) and by some hard blocks in SEM pictures (Figure 5). In this case, the secondary mesoporosity near p/p_0 0.45 can be attributed to interlamellar porosity.

The composition of the solid phase at different synthesis times during the pseudomorphic transformation of LiChrospher 60 is reported in Figure 8, as well as the yields of the incorporation of silica and surfactant in the solid (ratio between the amount in the solid and the amount in the synthesis gel). CTMA yield increases from 72% to 90% in the first 4 h, and the silica yield increases from 62% to 71%. This leads to an initial increase in CTMA/Si composition from 0.24 to 0.27. The increase in surfactant yield during the aging of MCM-41 has already been noticed in experiments performed at lower temperature and alkalinity.[37] This modification of the MCM-41 composition probably triggers the nucleation of the more favorable *Ia*3*d* mesostructure (MCM-48) under the present conditions. In an interesting parallel, in the thermodynamic CTAB/water phase diagram,[38] the cubic mesostructure is obtained for higher concentration of surfactant than the hexagonal mesostructure. The composition of MCM-48 is remarkably constant throughout the synthesis (CTMA/Si 0.27). Some decrease of the silica and surfactant yields observed after some aging (5 h) of MCM-48 could be attributed to the separation of some small crystals of the shell of MCM-48 beads resulting in the loss of a fraction of solid during the filtration. At the formation of the lamellar phase, the composition of the solid changes and approaches the composition found for the lamellar phase

(37) Galarneau, A.; Di Renzo, F.; Fajula, F.; Mollo, L.; Fubini, B.; Ottaviani, M. F. *J. Colloid Interface. Sci*. **1998**, *201*, 105.
(38) Auvray, X.; Petipas, C.; Anthore, R.; Rico, I.; Lattes, A. *J. Phys. Chem*. **1989**, *93*, 7458.

synthesized from nonporous silica (fumed silica) (CTMA/Si = 0.21). MCM-48 obtained through pseudomorphic synthesis combined with MCM-41/-48 phase transition appears as a surfactant-rich mesostructure with CTMA/Si = 0.27 as compared to MCM-41 (CTMA/Si = 0.24) and the lamellar structure (CTMA/Si = 0.21) (Figure 8).

Influence of the Parent Silica on the Phase Transformation Kinetics. The same sequence of phase formation (MCM-41 followed by MCM-48, followed in turn by the lamellar mesostructure) was observed when nonporous silica or the other parent porous silicas were used. However, the time scale of the process was different for the different sources of silica: 2 h of synthesis was enough to transform amorphous LiChrospher 60 into ordered MCM-48, whereas 4 h was necessary for nonporous silica. For the other sources of porous silica, it was observed that the induction time for phase formation strongly varied according to the silica source. A correlation was found between the transformation kinetics and the surface area of the parent porous silica. A diagram representing the mesostructures formed at each synthesis time as a function of the silica surface area of the parent porous silica is reported in Figure 9. Porous silicas with higher surface area lead to a faster MCM-41/-48 phase transformation. Around 10 h at a synthesis temperature of 150 °C is necessary to form MCM-48 starting from Hypersil (160 m^2/g), whereas only 2 h is required for LiChrospher 60 (740 m^2/g). Once MCM-48 is formed, it subsists as a stable phase in the reaction medium for ca. 10−12 h. As a consequence, the time at which the MCM-48/lamellar phase transformation is observed is affected in a similar way by the surface area of the starting silicas. For instance, the synthesis performed with LiChrospher 60 (740 m^2/g) gives the lamellar mesostructure after 15 h, whereas for the same synthesis time Hypersil (160 m^2/g) gives MCM-48.

In the MCM-41 pseudomorphic synthesis, the organic and inorganic components of the mesostructure are provided, respectively, by the diffusion of the surfactant inside the porosity of the silica beads and the dissolution of the primary nanoparticles constituting the parent silica beads. An amorphous silica with higher surface area presents smaller primary nanoparticles (Table 1) that can dissolve faster and provide a faster reprecipitation of the surfactant/silica mesostructure. As was described above, and was shown in detail in a previous study,[3] the pseudomorphic transformation of amorphous porous silica beads into MCM-41 is a progessive process where a poorly ordered and inhomogeneous mesostructure is initially produced and then rearranges gradually into a well-defined hexagonal mesostructure. This evolution of the initially formed silica/surfactant mesostructure can justify the different induction times for the formation of MCM-48: rapidly formed well-defined hexagonal MCM-41 (in equilibrium with its solution media) transforms faster in MCM-48.

Nonporous silica does not follow the same relationship between induction times of mesostructures formation versus surface area as porous silica (Figure 9). The transformation of the nanoparticles of the nonporous silica with 193 m^2/g is obtained after 4 h, whereas 9 h is necessary for a porous silica of similar surface area. This shorter induction time for

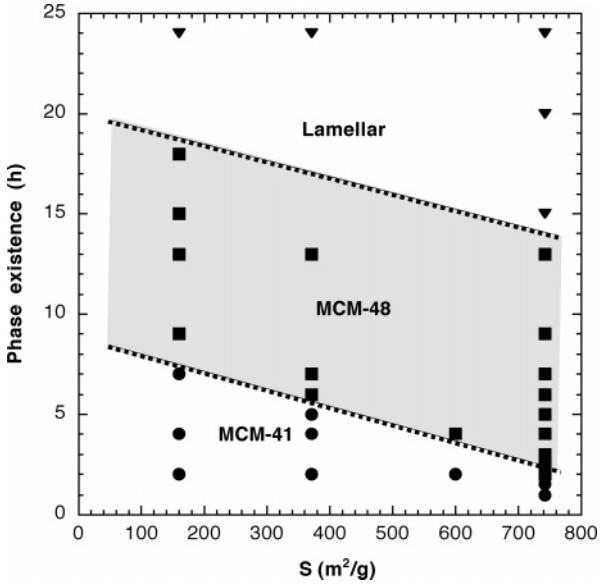

Figure 9. Domains of formation of (●) MCM-41, (■) MCM-48, and (▼) lamellar mesostructures as a function of synthesis time and surface area of the parent silica. The gray zone represents the MCM-48 domain.

nonporous silica comes from a difference of mechanism that is not occurring in a confined space as for porous silicas. As suggested by the SEM pictures (Figure 1), there is no morphology preservation during the different phase transitions for nonporous silica. The formation mechanism for nonporous silica of the different mesostructures undergoes a solution-mediated phase nucleation and growth. The phase transformation of nonporous silica is not constrained by diffusional limitations as in the case of the transformation of porous silica.

Heterogeneous Nucleation of MCM-41, Epitaxial Transformation of MCM-48, and Liquid Phase-Mediated Transformation for the Lamellar Phase. In which way can the kinetics of the pseudomorphic transformation shed some light on the mechanism of formation of each mesostructure? A mechanism of heterogeneous nucleation and of short-range transport inside the beads has been proposed for the pseudomorphic formation of MCM-41[3] and is supported by the influence of the surface area of the parent silica source on kinetics. Higher surface area parent silica will lead to faster well-defined MCM-41. The nucleation of MCM-41 occurs at the surface of the primary nanoparticles constituting the particle by their progressive dissolution and the reprecipitation with the surfactant present in the initial porosity.

In the case of the MCM-41/-48 phase transition, the mechanism could go through two possible mechanisms: cylinder merging or cylinder branching.[27] The cylinder-merging mechanism is reversible and kinetically favorable, while the cylinder-branching mechanism is thermodynamically more favorable but less reversible. Our results differ from the findings of Landry et al.,[27] in that no MCM-41/lamellar phase transition was observed prior to MCM-48 formation. This makes more likely that the phase transition in our conditions goes through a cylinder-branching mechanism (Figure 10) by epitaxial nucleation. The morphology preservation of the parent MCM-41 particles implies a solid-state transformation mechanism. In contrast, the outer crystals formed at the surface of some MCM-48 particles present a

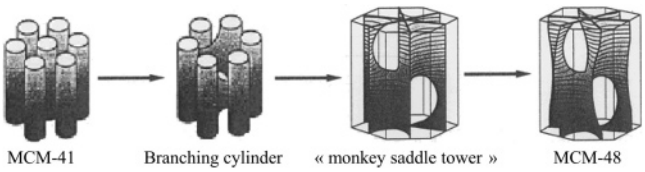

Figure 10. Schematic MCM-41/-48 phase transformation going through a cylinder-branching mechanism (adapted from ref 27).

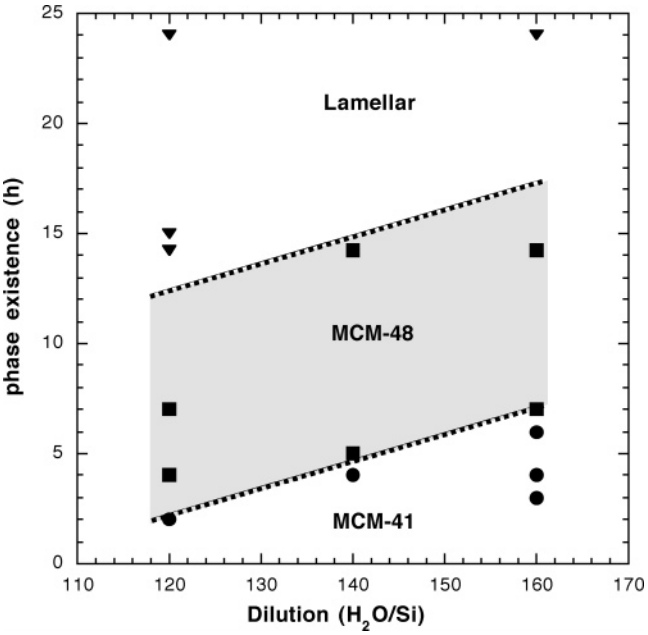

Figure 11. Domains of formation of (●) MCM-41, (■) MCM-48, and (▼) lamellar mesostructures as a function of synthesis time and dilution for LiChrospher 60 as parent silica. The gray zone represents the MCM-48 domain.

shape completely different from those present at the surface of some MCM-41 particles (Figure 5). The growth of smooth icosahedral crystals at the surface of MCM-48 particles has clearly taken place by another mechanism, implying the transport of species from the outer part of the particles through the solution creating some holes in the parent particles (Figure 6). It is very likely that the nucleation of this MCM-48 crystal shell is due to a transformation of the elongated crystals of MCM-41 already present at the outer surface of the particles (Figure 5), possibly by a local cylinder-branching mechanism. This would correspond to a possible mechanism of epitaxial nucleation of MCM-48, rapidly followed by a solution-mediated crystal growth. The MCM-48/lamellar phase transformation is certainly not a solid-state transformation mechanism, as no morphology and no surfactant/silica composition is conserved (Figures 5 and 8). The formation of the lamellar phase is due to its higher stability, which implies the dissolution of the less stable phase and is accompanied by a higher yield of silica. The nucleation of the lamellar phase is surely due to species in solution, and its growth follows a liquid phase-mediated mechanism, consecutively with the solution-mediated growth of the external crystals of MCM-48.

Particles Size Distribution. In our objective to generate materials for suitable chromatographic applications, the challenge was not only the preservation of the initial morphology of the parent silica, but also to avoid any aggregation between particles. The high alkalinity of the

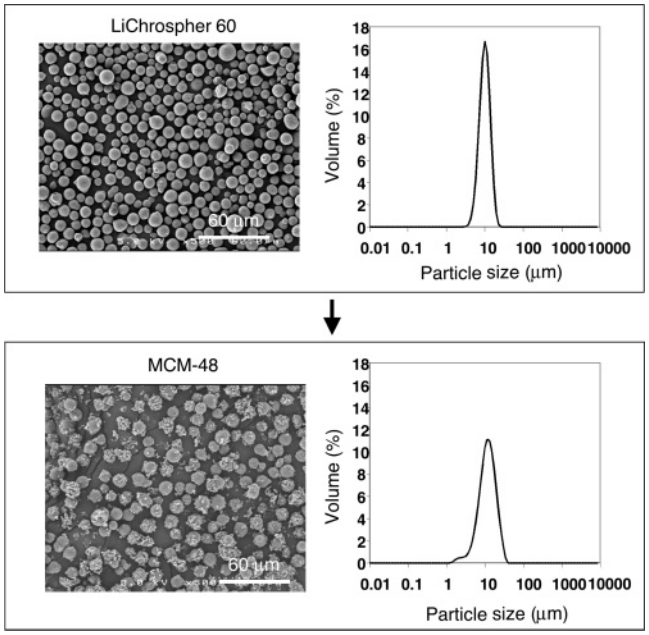

Figure 12. SEM pictures and particles size distributions of LiChrospher 60 and its transformation into MCM-48 for molar ratio in the synthesis of $1SiO_2/0.30NaOH/0.175CTAB/160H_2O$.

synthesis media, the high-temperature synthesis, and the low amount of water necessary for MCM-48 synthesis are, from our knowledge on MCM-41 pseudomorphic synthesis, unfavorable to avoid particle aggregation due to a fast kinetic of MCM-41 formation. Therefore, particles size distribution of MCM-48 materials obtained from the different sources of porous silica shows some aggregation. For example, MCM-48 particles synthesized from LiChrospher 60 as the parent silica show some aggregation resulting in a maximum in the particle size distribution at 24 μm instead of 12 μm as in the parent silica, as well as the contribution of some small particles of ca. 4 μm (not shown). The presence of small particles comes from small aggregates of smooth icosahedral particles dissociated from the shell of the particle. The aggregation between particles is not dependent on synthesis time; the aggregation of the particles is observed from the very beginning of the reaction (1 h) when MCM-41 particles are first formed. This behavior has been observed for all sources of parent silica. In a first attempt, to control particles aggregation, the alkalinity of the solution has been decreased from NaOH/Si = 0.38 to NaOH/Si = 0.30. The particles aggregation decreases but remains noticeable in the particle size distribution. In previous MCM-41 pseudomorphic synthesis work, another parameter that proved crucial to avoiding particle aggregation was the dilution.[3] Indeed, a larger amount of water in the pseudomorphic synthesis of MCM-41 led to nonaggregated particles by slowing down the kinetics of formation. Therefore, in the present study, the amount of water was increased progressively from $H_2O/Si = 120$ to $H_2O/Si = 160$, keeping the lower alkalinity conditions (NaOH/Si = 0.30). The induction time for the nucleation of MCM-48 was increased, indicating that, as expected, dilution slows down the kinetics of formation of the MCM-41 precursor. Using LiChrospher 60 as the parent silica, a minimum of 7 h was then required to obtain MCM-48 mesostructure with $H_2O/Si = 160$, while

only 4 h was necessary with $H_2O/Si = 120$ (Figure 11). As noticed under the previous synthesis conditions (higher alkalinity and lower amount of water), once MCM-48 is formed, it subsists as a stable mesostructure for ca. 10 h before the lamellar mesostructure forms. Particle size distributions of MCM-48 mesostructures synthesized from LiChrospher 60 with $H_2O/Si = 160$ (Figure 12) show that the dilution actually allowed one to avoid the aggregation between particles leading to narrow particle size distribution with a maximum centered at 13 μm in accordance with the parent silica. Besides, the dilution minimizes the formation of the shell on the outer surface of the particles, minimizing also the amount of fine particles in the particle size distribution. By slowing down the whole process, the dilution prevents the contribution of Ostwald ripening (outside nucleation) in the MCM-41 precursor and as a consequence the formation of the shell on MCM-48 particles. Discrete and nonaggregated particles of MCM-48 have been obtained under these optimized conditions corresponding to the following gel composition: $1SiO_2/0.30NaOH/0.175CTAB/160H_2O$.

Conclusion

The synthesis of micrometer-sized spherical particles of MCM-48 has been achieved through a MCM-41 pseudomorphic synthesis procedure using preformed porous silica beads as silica source combined with a MCM-41/-48 phase transition. The morphology of the parent silica source is preserved all along the reaction. The MCM-41/-48 transition is possible thanks to the low polymerization state of the silica in the transient hexagonal mesostructure because of the high alkalinity of the synthesis medium. MCM-48 appears as a surfactant-rich metastable mesostructure between MCM-41 mesostructures obtained at short synthesis time and a lamellar mesostructure obtained at longer synthesis time. The kinetics of MCM-48 formation is strongly dependent on the surface area of the parent silica. A parent silica with higher surface area produces MCM-48 mesostructure in shorter synthesis time. The mechanism of the MCM-41/-48 phase transition is consistent with an epitaxial nucleation, through a solid-state mechanism, whereas the formation of the consecutive lamellar phase is more probably the result of nucleation from the solution.

From a practical point of view, these results provide a workable strategy to produce MCM-48 mesostructures with any particle shape and size, and particularly as spherical beads. Furthermore, the kinetic phases diagrams revealed by this study allow one to predict the synthesis time required for the formation of MCM-48 mesostructures from any source of porous silicas.

Acknowledgment. We thank the European Commission for funding this work under the GROWTH-INORGPORE program (project number G5RD-CT-2000-00317). Authors also thank Didier Cot for the SEM pictures.

CM050068J